FINE-TUNING ELECTRODE INFORMATION IN ELECTRICAL IMPEDANCE TOMOGRAPHY

JÉRÉMI DARDÉ*, HARRI HAKULA†, NUUTTI HYVÖNEN‡, AND STRATOS STABOULIS§

Abstract. Electrical impedance tomography is a noninvasive imaging technique for recovering the admittance distribution inside a body from boundary measurements of current and voltage. In practice, impedance tomography suffers from inaccurate modelling of the measurement setting: The exact electrode locations and the shape of the imaged object are not necessarily known precisely. In this work, we tackle the problem with imperfect electrode information by introducing the Fréchet derivative of the boundary measurement map of impedance tomography with respect to the electrode shapes and locations. This enables us to include the fine-tuning of the information on the electrode positions as a part of a Newton-type output least squares reconstruction algorithm; we demonstrate that this approach is feasible via a two-dimensional numerical example based on simulated data. The impedance tomography measurements are modelled by the complete electrode model, which is in good agreement with real-life electrode measurements.

Key words. electrical impedance tomography, Fréchet derivative, domain derivative, model inaccuracies, output least squares, complete electrode model

AMS subject classifications. 35R30, 35J25, 65N21

1. Introduction.

In *electrical impedance tomography* (EIT), electric current is conducted into a physical body, the resulting potential is measured on the boundary, and the obtained data is used to gather information about the conductivity distribution inside the object of interest. EIT can be used in medical imaging, geophysics, environmental sciences, nondestructive testing of materials and process tomography; consult the review articles [2, 4, 36] and the references therein for more details about the potential applications of EIT.

In mathematical analysis of EIT, it is usually assumed that one can specify the current density on all of the object boundary and measure the resulting boundary potential everywhere (cf., e.g., [36]). However, when performing real-world EIT measurements, one can only control the net currents through a finite number of electrodes and measure the resulting electrode potentials. Currently, the best model for such realistic measurements is the *complete electrode model* (CEM), which takes into account electrode shapes and contact impedances at electrode-object interfaces. The CEM is capable of predicting real-life measurements up to measurement precision [5, 35].

To make matters more complicated, a real-life measurement setting of EIT often contains more unknowns than the conductivity distribution: The exact electrode shapes and locations, the contact impedances and the outer boundary shape of the imaged object are not necessarily known accurately. (As an example, consider a medical application where the body shape and the contact impedances vary from patient

*Department of Mathematics and Systems Analysis, Aalto University, P.O. Box 11100, FI-00076 Aalto, Finland (jeremi.darde@tkk.fi).

†Department of Mathematics and Systems Analysis, Aalto University, P.O. Box 11100, FI-00076 Aalto, Finland (harri.hakula@tkk.fi).

‡Department of Mathematics and Systems Analysis, Aalto University, P.O. Box 11100, FI-00076 Aalto, Finland (nuutti.hyvonen@hut.fi). The work of N. Hyvönen was supported by the Finnish Funding Agency for Technology and Innovation TEKES (contract 40370/08) and the Academy of Finland (the Centre of Excellence in Inverse Problems Research and projects 135979 and 141044).

§Department of Mathematics and Systems Analysis, Aalto University, P.O. Box 11100, FI-00076 Aalto, Finland (stratos.staboulis@tkk.fi). The work of S. Staboulis was supported by the Academy of Finland (the Centre of Excellence in Inverse Problems Research and project 141044).

to patient and the placement of the electrodes cannot always be localized accurately.) These kinds of inaccuracies are a considerable hindrance for establishing EIT as a practical imaging modality since it is well known that even slight mismodelling can quite easily ruin the reconstruction of the conductivity completely [1, 3, 24, 34] — especially if difference data, i.e., measurements of the same object at two different time instances, are not available.

In this work, we pave the way for including the fine-tuning of the information on the electrode shapes and locations as a part of an iterative Newton-type output least squares reconstruction algorithm of EIT; see, e.g., [21, 27, 28] for examples of Newton-based techniques aiming at the determination of the mere conductivity distribution in the framework of the CEM. The first step in building such an extended reconstruction method is to show that the measurement map of the CEM is Fréchet differentiable with respect to the electrodes, which is what we establish with the help of techniques stemming from [25, 13, 15]. We want to emphasize, however, that the standard methodology of shape estimation within EIT does not trivially generalize to our framework: Most of the existing algorithms consider estimating shapes of geometric entities lying well within the body, i.e., at a distance from the outer boundary. This provides workspace inside the object of interest without affecting the boundary where the measurements are carried out, which in turn allows to express the needed Fréchet derivatives as boundary values of solutions to elliptic boundary value problems with source terms located away from the outer boundary (cf., e.g., [15, 20]). Here, the needed perturbations of the electrodes affect the measurements more directly, resulting in distributional boundary sources on the electrodes in the elliptic problem that defines the corresponding Fréchet derivative.

We justify the need for differentiation with respect to the electrode locations by introducing, within the Bayesian paradigm [22], a Newton-type output least squares algorithm that simultaneously reconstructs the internal conductivity distribution and the electrode locations in a two-dimensional measurement geometry, assuming that the lengths of the electrodes are known. The functionality of the method is demonstrated by a numerical experiment based on simulated noisy data. In particular, it is shown that ignoring the incompleteness of the information on the electrode positions gives an intolerably bad reconstruction of the conductivity, whereas including the location search of the electrodes as a part of the algorithm provides almost as good results as knowing the exact locations to begin with.

We also want to point out that the ability to differentiate the CEM measurement map with respect to the electrodes will also be useful for other practical purposes: If one considers including the fine-tuning of the information on the object boundary shape as a part of an output least squares algorithm, one ends up dealing with perturbations of the boundary that also stretch the electrodes, and thus it is natural to allow the reconstruction method to compensate for such deformations by being able to independently reshape the electrodes, as well (see [8]). Moreover, our Fréchet differentiability results should be of aid if the objective is to determine the most informative positions for the available electrodes based on prior information about the imaged object (cf. [16]).

To put our ideas into perspective, let us survey some earlier studies tackling the uncertainties in the locations of the electrodes, the contact impedances and the shape of the object boundary in the framework of EIT. First of all, the idea of simultaneous localization of the electrodes and reconstruction of the conductivity distribution has been previously considered in [34], where the authors do not, however, calculate the

Fréchet derivatives with respect to the electrode locations explicitly but use numerical difference approximations (see [34, (5)]). Moreover, differentiation with respect to the shapes of the electrodes is not considered in [34]. Similar considerations can also be found in [16] where optimal experimental design is tackled. Simultaneous reconstruction of the internal conductivity distribution and the contact impedances at the electrode-object interfaces has been considered in [12, 37] and many other papers since. On the other hand, the approximation error methodology has been successfully employed to obtain reconstructions of the conductivity in case the measurement setting is modelled inaccurately [30, 31, 32]: The leading idea is to use numerical simulations together with prior information about the unknown parameters to approximate and store the statistics of the inaccuracies caused by the mismodelling in advance. This knowledge is then utilized in handling the modelling errors, essentially, in the same way as the measurement noise in some Bayesian inversion algorithm (cf., e.g., [22]). Another successful approach for coping with an unknown object boundary was suggested by Kolehmainen, Lassas and Ola in [23]. Their method is based on allowing slightly anisotropic conductivities and on the use of sophisticated mathematical instruments such as quasiconformal maps and Teichmüller spaces.

This text is organized as follows. Section 2 introduces the CEM forward model and Section 3 a general way of perturbing the corresponding electrodes. The main theoretical results are presented in Section 4. Subsequently, Section 5 considers technical issues related to perturbation of the CEM measurement setting by a wide class of diffeomorphisms, and the actual proofs of the main differentiability results can be found in Section 6. Section 7 contains the numerical experiments. Finally, in Section 8 we list the concluding remarks.

2. Complete electrode model. Let $\Omega \subset \mathbb{R}^n$, $n = 2$ or 3, be a bounded domain and assume that its boundary $\partial\Omega$ is an orientable C^∞-manifold. We denote by $\sigma\colon \Omega \to \mathbb{C}^{n\times n}$ the electrical admittance distribution of Ω and assume that it satisfies the following, physically reasonable conditions [2]:

$$\sigma = \sigma^{\mathrm{T}}, \qquad \mathrm{Re}\,(\sigma\xi\cdot\overline{\xi}) \geq \varsigma_1|\xi|^2, \qquad |\sigma\xi\cdot\overline{\xi}| \leq \varsigma_2|\xi|^2 \tag{2.1}$$

for some constants $\varsigma_1, \varsigma_2 > 0$ and for all $\xi \in \mathbb{C}^n$ almost everywhere in Ω.

Assume that the boundary $\partial\Omega$ is partially covered with $M \in \mathbb{N}\setminus\{1\}$ well-separated, open, bounded and connected electrodes $\{E_m\}_{m=1}^M$, which are identified with the parts of $\partial\Omega$ that they cover. The electrodes are modelled as ideal conductors and for the sake of simplicity we assume that their boundaries are smooth. The union of the electrodes is denoted by $E = \cup_m E_m \subset \partial\Omega$, and the time-harmonic electrode net currents and voltage patterns by the vectors $I = [I_m]_{m=1}^M$ and $U = [U_m]_{m=1}^M$ of $\mathbb{C}^M$, respectively, where $I_m, U_m \in \mathbb{C}$ correspond to the measurements on the mth electrode. Due to to the current conservation law, I actually belongs to the subspace $\mathbb{C}^M_\diamond \subset \mathbb{C}^M$ consisting of those vectors whose components have vanishing sum. The contact impedances (cf. [5]) that characterize the thin and highly resistive layers at the electrode-object interfaces are modelled by $z \in \mathbb{C}^M$ that is assumed to satisfy $\mathrm{Re}\,z_j \geq c > 0$ for $j = 1, \ldots, M$.

According to the CEM [5, 35], the pair $(u, U) \in \mathcal{H}^1 := \left(H^1(\Omega)\oplus\mathbb{C}^M\right)/\mathbb{C}$, composed of the electromagnetic potential within Ω and the voltages on the electrodes, is

the unique solution of the elliptic boundary value problem

$$\begin{aligned} &\nabla\cdot\sigma\nabla u = 0 && \text{in } \Omega,\\ &\nu\cdot\sigma\nabla u = 0 && \text{on } \partial\Omega\setminus\overline{E},\\ &u + z_m\nu\cdot\sigma\nabla u = U_m && \text{on } E_m,\quad m=1,\dots,M,\\ &\int_{E_m}\nu\cdot\sigma\nabla u\,dS = I_m, && m=1,\dots,M, \end{aligned} \tag{2.2}$$

for a given electrode current pattern $I\in\mathbb{C}^M_\diamond$ and with $\nu=\nu(x)$ denoting the exterior unit normal of $\partial\Omega$. The definition of $\mathcal{H}^1$ as a quotient space emphasizes the freedom in the choice of the ground level of potential; in other words, one can never measure absolute potentials, only potential differences.

The weak formulation of the CEM forward problem (2.2) is to find $(u,U)\in\mathcal{H}^1$ that satisfies [35]

$$B\big\{(u,U),(v,V)\big\} = \sum_{m=1}^M I_m\overline{V}_m \qquad \text{for all } (v,V)\in\mathcal{H}^1, \tag{2.3}$$

where the sesquilinear form $B\colon \mathcal{H}^1\times\mathcal{H}^1\to\mathbb{C}$ is defined by

$$B\big\{(u,U),(v,V)\big\} = \int_\Omega \sigma\nabla u\cdot\nabla\overline{v}\,dx + \sum_{m=1}^M \frac{1}{z_m}\int_{E_m}(U_m-u)(\overline{V}_m-\overline{v})\,dS. \tag{2.4}$$

The following proposition states that B is concordant with the natural quotient norm of $\mathcal{H}^1$ defined by

$$\|(v,V)\|_{\mathcal{H}^1} = \inf_{c\in\mathbb{C}}\Big\{\|v-c\|^2_{H^1(\Omega)} + \sum_{m=1}^M |V_m-c|^2\Big\}^{1/2}.$$

As the proposition is only a slight modification of [17, Corollary 2.6], its proof is omitted.

PROPOSITION 2.1. *The sesquilinear form $B\colon \mathcal{H}^1\times\mathcal{H}^1\to\mathbb{C}$ is bounded and coercive with respect to the norm $\|\cdot\|_{\mathcal{H}^1}$, that is*

$$\begin{aligned} \big|B\big\{(u,U),(v,V)\big\}\big| &\le C_1\|(u,U)\|_{\mathcal{H}^1}\|(v,V)\|_{\mathcal{H}^1},\\ \operatorname{Re} B\big\{(v,V),(v,V)\big\} &\ge C_2\|(v,V)\|^2_{\mathcal{H}^1} \end{aligned}$$

for all $(u,U),(v,V)\in\mathcal{H}^1$ and some $0<C_1,C_2<\infty$ that can be chosen independently of the electrode configuration if the electrodes are known to satisfy

$$\min_{1\le m\le M}|E_m| \ge c \tag{2.5}$$

for some fixed $c>0$.

The unique solvability of (2.2) can be proved by combining Proposition 2.1 and the obvious boundedness of the antilinear functional on the right-hand side of (2.3) with the Lax–Milgram lemma [17, 35]. This procedure also provides the estimate

$$\|(U,u)\|_{\mathcal{H}^1} \le\ C|I|, \tag{2.6}$$

where the constant of continuity $C = C(\Omega, \sigma, z)$ can again be chosen independently of the electrodes if it is assumed that (2.5) holds (cf., e.g., [11, (2.4)]).

An ideal measurement corresponding to the CEM provides the electrode voltages $U \in \mathbb{C}^M/\mathbb{C}$ for some applied current pattern $I \in \mathbb{C}^M_\diamond$. For a given measurement setting $\{\Omega, E, \sigma, z\}$, we thus define the measurement operator $R\colon \mathbb{C}^M_\diamond \to \mathbb{C}^M/\mathbb{C}$ by

$$R : I \mapsto U. \tag{2.7}$$

Obviously, R is linear and bounded (cf. (2.2) and (2.6)), with a constant of continuity that can be chosen independently of the electrode configuration under the assumption (2.5).

REMARK 1. *The pair $(u, U) \in \mathcal{H}^1$ is referred to as the* background solution. *For smooth σ, it holds that $\nu \cdot \sigma \nabla u|_E \in H^1(E)$, $\nu \cdot \sigma \nabla u|_{\partial\Omega} \in H^{1/2-\epsilon}_\diamond(\partial\Omega)$ and $u \in H^{2-\epsilon}(\Omega)/\mathbb{C}$ for all $\epsilon > 0$. Indeed, the first inclusion is a consequence of [11, Lemma 3.1], which in turn means that the other two follow from the properties of the zero extension in Sobolev spaces [29, Chapter 1, Theorem 11.4] and the regularity theory for elliptic partial differential equations [29, Chapter 2, Remark 7.2], respectively.*

3. Electrode perturbation. In this section, we will introduce a general way of perturbing the electrodes $\{E_m\}_{m=1}^M$ with the help of C^1 vector fields living on ∂E; if $n = 2$, you may just think of collections of vectors at the end points of the electrodes. To this end, we denote by

$$\mathcal{B}_d \,=\, \{a \in C^1(\partial E, \mathbb{R}^n) \mid \|a\|_{C^1(\partial E, \mathbb{R}^n)} < d\}$$

the origin-centered open ball of radius $d > 0$ in the topology of $C^1(\partial E, \mathbb{R}^n)$. Furthermore, we let $B_d(x) = \{z \in \mathbb{R}^n \mid |z - x| < d\}$ be a standard open ball in $\mathbb{R}^n$, and for small enough $d > 0$ we define

$$P_x : B_d(x) \to \partial\Omega$$

to be the (nonlinear) projection that maps $y \in \mathbb{R}^n$, which lies sufficiently close to $x \in \partial E$, in the direction of $\nu(x)$ onto $\partial\Omega$. To be quite precise, there may be several points on $\partial\Omega$ satisfying these conditions, and thus we enhance the definition of P_x by requiring that $P_x x = x$ and P_x is continuous. It is obvious that P_x is well defined for some $d = d(\Omega) > 0$ that can be chosen independently of $x \in \partial E$ due to a compactness argument.

For a vector field $a \in \mathcal{B}_d$ we define a perturbed set of electrodes, or more precisely the corresponding boundaries via

$$\partial E^a_m \,=\, \{z \in \partial\Omega \mid z = P_x(x + a(x)) \text{ for some } x \in \partial E_m\}, \qquad m = 1, \ldots, M.$$

The following proposition shows that $\{E^a_m\}_{m=1}^M$ really are reasonable electrodes for small enough $d > 0$. The assertion is formulated exclusively for $n = 3$, but the analogous, slightly simpler result also holds in two dimensions, where the boundary of an electrode consists of only two points.

PROPOSITION 3.1. *There exists $d > 0$ such that for any $a \in \mathcal{B}_d$ the sets ∂E^a_m, $m = 1, \ldots, M$, are C^1-curves bounding well-separated, open, bounded and connected electrodes $E^a_m \subset \partial\Omega$, $m = 1, \ldots, M$. Moreover, the mapping*

$$F[a] : x \mapsto P_x(x + a(x)), \quad \partial E \to \partial E^a := \cup_{m=1}^M \partial E^a_m \tag{3.1}$$

is a C^1-diffeomorphism.

Proof. Fix $m \in \mathbb{N}$ between 1 and M. Let $U \subset \mathbb{R}^2$ be an open set containing the origin such that there exists a local parametrization $\vartheta(\xi)$, $\xi \in U$, of $\partial\Omega$ in a neighborhood of $\vartheta(0) = x \in \partial E_m$. As a smooth one-dimensional manifold, ∂E_m can be locally given in the form of a smooth unit speed curve $\{\gamma(s) \mid s \in (-l, l),\, \gamma(0) = x\}$, where $l > 0$.

Consider a function $G\colon C^1(\partial E_m, \mathbb{R}^3) \times (-l, l) \times \mathbb{R} \times U \to \mathbb{R}^3$ defined by the formula

$$G(a, s, \alpha, \xi) = \gamma(s) + a(\gamma(s)) + \alpha\nu(\gamma(s)) - \vartheta(\xi). \tag{3.2}$$

Obviously G is continuously Fréchet differentiable with respect to each of the four variables. In particular, the derivative of G can be written in the form

$$G'(a, s, \alpha, \xi) = \begin{bmatrix} * & * & \nu(\gamma(s)) & -J_\vartheta(\xi) \end{bmatrix} \tag{3.3}$$

where J_ϑ is the Jacobian matrix of the local parametrization ϑ and the symbol $*$ replaces the entries that are not needed in the following calculations.

We observe from (3.2) that $G(\mathbf{0}) = 0$ and define a linear transformation $A\colon \mathbb{R} \times \mathbb{R}^2 \to \mathbb{R}^3$ by $A : (\beta, \omega) \mapsto \beta\nu(x) - J_\vartheta(0)\omega$. Since $J_\vartheta(0)\colon \mathbb{R}^2 \to T_x\partial\Omega$, where $T_x\partial\Omega$ is the tangent plane of $\partial\Omega$ at x, is an isomorphism and $\nu(x) \perp T_x\partial\Omega$, we conclude that A is also an isomorphism. In consequence, the Banach space version of the implicit function theorem tells us that there exists an open neighborhood of the origin $\mathbf{0}$

$$V = V_1 \times V_2 \times V_3 \times V_4 \subset C^1(\partial E_m, \mathbb{R}^3) \times (-l, l) \times \mathbb{R} \times U$$

and continuously Fréchet differentiable functions $\widetilde{\alpha}\colon V_1 \times V_2 \to \mathbb{R}$ and $\widetilde{\xi}\colon V_1 \times V_2 \to \mathbb{R}^2$ such that $G(a, s, \alpha, \xi) = 0$ for $(a, s, \alpha, \xi) \in V$, if and only if $\alpha = \widetilde{\alpha}(a, s)$ and $\xi = \widetilde{\xi}(a, s)$.

Due to the definition of G, it is obvious that the C^1-map

$$\gamma_a : s \mapsto \vartheta\big(\widetilde{\xi}(a, s)\big) = \gamma(s) + a(\gamma(s)) + \widetilde{\alpha}(a, s)\nu(\gamma(s)) \tag{3.4}$$

provides a local parametrization of ∂E_m^a around $P_x(x + a(x)) \in \partial E_m^a$. Moreover, since $\widetilde{\alpha}(\cdot, \cdot)$ is continuous and clearly $\widetilde{\alpha}(0, \cdot) \equiv 0$, a straightforward differentiation shows that $|\gamma_a'(0)| \geq c(d) > 0$ for $a \in \mathcal{B}_d$ with sufficiently small $d > 0$. In particular, as the derivative of γ_a does not vanish in a neighborhood of the origin, the inverse of γ_a, defined in some neighborhood of $P_x(x + a(x))$ on ∂E_m^a, is also a C^1-mapping.

By constructing such a local and injective parametrization of ∂E_m^a for each $x \in \partial E_m$, and then using compactness to build a global, injective and surjective, parametrization of ∂E_m^a by glueing together a finite number of such local parametrizations, it follows that ∂E_m^a is C^1-boundary of an open, bounded and connected electrode E_m^a and that $F[a]$ is a C^1-diffeomorphism between ∂E_m and ∂E_m^a for all $a \in \mathcal{B}_d$ with sufficiently small $d > 0$. This procedure can be carried out separately for each $m = 1, \ldots, M$, and finally, by decreasing $d > 0$ if necessary, it can be concluded that E_m^a, $m = 1, \ldots, M$, are well-separated. This completes the proof. ∎

In what follows, we will implicitly assume that $d > 0$ is small enough for Proposition 3.1 to hold.

4. Main result. In this section, our main results are formulated exclusively for the three-dimensional case, i.e., for $n = 3$. This will also be the setting of Sections 5 and 6 below. We want to emphasize, however, that the two-dimensional case is more straightforward and can be handled using similar techniques (cf. Section 7). For the sake of simplicity we assume that $\sigma \in C^\infty(\overline{\Omega}, \mathbb{C}^{n\times n})$ in the following.

Due to the electrode boundary perturbation introduced in the previous section, the measurement map of CEM, defined originally by (2.7), can be considered as an operator of two variables, namely

$$R : (a, I) \mapsto U[a], \quad \mathcal{B}_d \times \mathbb{C}^M_\diamond \to \mathbb{C}^M/\mathbb{C},$$

where $U[a]$ is the electrode potential component of the solution $(u[a], U[a]) \in \mathcal{H}^1$ to (2.2) when the original electrodes $\{E_m\}_{m=1}^M$ are replaced by the perturbed ones $\{E_m^a\}_{m=1}^M$ from Proposition 3.1. Obviously, R is linear in its second variable but nonlinear in the first one; in the following, we will give an explicit representation of the Fréchet derivative of R with respect to the first variable at the origin.

Let us introduce a family of distributions $\{\delta_m\}_{m=1}^M \subset H^{-1/2-\epsilon}(\partial\Omega)$, $\epsilon > 0$, defined through

$$\langle \delta_m, v\rangle_{\partial\Omega} = \int_{\partial E_m} v\, ds, \qquad v \in H^{1/2+\epsilon}(\partial\Omega),$$

for $m = 1, \ldots, M$. Notice that any $v \in H^{1/2+\epsilon}(\partial\Omega)$, $\epsilon > 0$, has a well defined restriction $v|_{\partial E} \in H^\epsilon(\partial E)$ due to the trace theorem, and thus the definition of the family $\{\delta_m\}_{m=1}^M$ is unambiguous. Moreover, we denote the characteristic function of $E_m \subset \partial\Omega$ by χ_m, $m = 1, \ldots, M$, and the unit exterior normal of ∂E in the tangent bundle of $\partial\Omega$ by $\nu_{\partial E}$. Let us then introduce a new boundary value problem for a generic interior potential and electrode voltage pair (v, V):

$$\begin{aligned}
&\nabla \cdot \sigma \nabla v = 0 && \text{in } \Omega,\\
&\nu \cdot \sigma \nabla v - \sum_{m=1}^M \frac{1}{z_m}\big((V_m - v)\chi_m + (a_\tau \cdot \nu_{\partial E})(U_m - u)\delta_m\big) = 0 && \text{on } \partial\Omega,\\
&\int_{E_m} (V_m - v)\, dS + \int_{\partial E_m} (a_\tau \cdot \nu_{\partial E})(U_m - u) ds = 0, && m = 1, \ldots, M,
\end{aligned} \tag{4.1}$$

where $a_\tau := a - (a \cdot \nu)\nu$ is the tangential component of $a \in C^1(\partial E, \mathbb{R}^n)$ with respect to $\partial\Omega$ and $(u, U) = (u[0], U[0]) \in \mathcal{H}^1$ is the background solution, i.e., the solution of (2.2) for a given $I \in \mathbb{C}^M_\diamond$. It turns out that (4.1) has a unique solution $(u'[a], U'[a])$ in $\mathcal{H}^{1-\varepsilon} := \big(H^{1-\epsilon}(\Omega) \oplus \mathbb{C}^M\big)/\mathbb{C}$ with $\epsilon > 0$ — the proof is postponed to Section 6 — and that the second component of this solution, i.e., $U'[a]$, defines the Fréchet derivative of R with respect to its first variable, as concretized by the following theorem.

THEOREM 4.1. *The measurement operator $R : \mathcal{B}_d \times \mathbb{C}^M_\diamond \to \mathbb{C}^M/\mathbb{C}$ is Fréchet differentiable with respect to the first variable at the origin, i.e.,*

$$\lim_{a\to 0} \frac{1}{\|a\|_{C^1(\partial E, \mathbb{R}^n)}} \|R[a] - R[0] - R'a\|_{\mathcal{L}(\mathbb{C}^M_\diamond, \mathbb{C}^M/\mathbb{C})} = 0,$$

where the bilinear Fréchet derivative $R' : C^1(\partial E, \mathbb{R}^n) \times \mathbb{C}^M_\diamond \to \mathbb{C}^M/\mathbb{C}$ is defined through

$$R' : (a, I) \mapsto U'[a], \tag{4.2}$$

with $U'[a]$ being the second component of the solution to (4.1).

At first sight it may seem that Theorem 4.1 is not very practical as it defines the Fréchet derivative of R with the help of a boundary value problem that does not fall within the framework of H^1-based variational theory. In particular, it is not obvious

how to solve (4.1) by standard finite element methods. Fortunately, there exists also a dual approach for sampling the Fréchet derivative.

COROLLARY 4.2. *Let $(\tilde{u}, \tilde{U}) \in \mathcal{H}^1$ be the solution of (2.2) for some electrode current pattern $\tilde{I} \in \mathbb{C}^M_\diamond$. Then, for any $(a, I) \in C^1(\partial E, \mathbb{R}^n) \times \mathbb{C}^M_\diamond$ it holds that*

$$\sum_{m=1}^{M} (R'(a, I))_m \tilde{I}_m = -\sum_{m=1}^{M} \frac{1}{z_m} \int_{\partial E_m} (a_\tau \cdot \nu_{\partial E})(U_m - u)(\tilde{U}_m - \tilde{u}) ds, \tag{4.3}$$

where (u, U) is the background solution, i.e., the solution of (2.2) corresponding to $I \in \mathbb{C}^M_\diamond$.

Theorem 4.1 and Corollary 4.2 are the main results of this work. Sections 5 and 6 below are devoted to proving them and showing that all the related definitions are unambiguous.

5. Convergence lemmas. In order to analyze the perturbations of the domain Ω needed when proving Theorem 4.1, let us introduce some mathematical concepts following the guidelines in [9]. The space of k times continuously differentiable vector fields whose partial derivatives of order $0 \le j \le k$ vanish at infinity is denoted by $C^k_0(\mathbb{R}^n, \mathbb{R}^n)$; take note that $C^k_0(\mathbb{R}^n, \mathbb{R}^n)$ is a Banach space when equipped with the natural norm (cf. [9, p. 68]). Furthermore, let us introduce the family of diffeomorphisms

$$\mathcal{F}^k_0 = \left\{ F \colon \mathbb{R}^n \to \mathbb{R}^n \;\middle|\; F - \mathrm{id} \in C^k_0(\mathbb{R}^n, \mathbb{R}^n) \text{ and } F^{-1} \in C^k(\mathbb{R}^n, \mathbb{R}^n) \right\},$$

where id denotes the identity map, and its subfamily

$$\mathcal{G}^k(\Omega) = \left\{ F \in \mathcal{F}^k_0 \;\middle|\; F(\Omega) = \Omega \right\},$$

where Ω is as defined in Section 2. The following theorem gives us the freedom to consider the perturbations of the electrode boundaries introduced in Section 3 as elements of $\mathcal{G}^1(\Omega)$.

THEOREM 5.1. *There exists $d > 0$ such that for any $a \in \mathcal{B}_d$ the map of (3.1) can be extended to be an element of $\mathcal{G}^1(\Omega)$, denoted still by $F[a]$, in such a way that*

$$\|F[a] - \mathrm{id}\|_{C^1(\mathbb{R}^n, \mathbb{R}^n)} \le C \|a\|_{C^1(\partial E, \mathbb{R}^n)}, \tag{5.1}$$

for some constant $C = C(d, \Omega) > 0$ that is independent of a.

Proof. To begin with, notice that it follows straightforwardly from the proof of Proposition 3.1 that

$$\|F[a] - \mathrm{id}\|_{C^1(\partial E, \mathbb{R}^n)} \le C \|a\|_{C^1(\partial E, \mathbb{R}^n)} \tag{5.2}$$

for all $a \in \mathcal{B}_d$, with sufficiently small $d > 0$, and with $C > 0$ that is independent of a. Indeed, by differentiating $G(a, s, \tilde{\alpha}, \tilde{\xi}) = 0$ with respect to s, one easily sees that not only $\tilde{\alpha}(a, s)$ is continuously Fréchet differentiable with respect to a for $(a, s) \in V_1 \times V_2$ but the same also holds for the derivative of $\tilde{\alpha}(a, s)$ with respect to s. Hence, the claim follows from the local parametrization (3.4) of $F[a]$, the Lagrange mean value theorem for Banach spaces, and the fact that $\tilde{\alpha}(0, s)$ is identically zero for $s \in V_2$.

With the help of tubular neighborhoods of the electrode boundaries, we extend $F[a] : \partial E \to \partial E^a$ to a C^1-mapping $F[a] : \partial\Omega \to \partial\Omega$ so that (5.2) continues to hold with the norm of $C^1(\partial E, \mathbb{R}^n)$ on the left-hand side replaced by that of $C^1(\partial\Omega, \mathbb{R}^n)$ and possibly with some different constant $C > 0$, which is still independent of a. By

using local coordinates on $\partial\Omega$ and an argument similar to that on page 78 of [9], it follows that for a small enough $d > 0$ the extended $F[a]$ is a C^1-diffeomorphism of $\partial\Omega$ to itself for any $a \in \mathcal{B}_d$.

To complete the proof, we extend the vector field $F[a] - \mathrm{id}$ to an element of $C_0^1(\mathbb{R}^n, \mathbb{R}^n)$ so that (5.1) is satisfied for some $C > 0$ and all $a \in \mathcal{B}_d$. Repeating the argumentation of [9, p. 78] enables us to choose $d > 0$ small enough so that $F[a] : \mathbb{R}^n \to \mathbb{R}^n$ is bijective and its inverse is continuously differentiable for any $a \in \mathcal{B}_d$. □

In the remainder of this section, we will analyze the behavior of the CEM when the electrodes are deformed by a general element of $\mathcal{G}^1(\Omega)$; the particular diffeomorphism of Theorem 5.1 will move into the focus of our attention in Section 6 below. To be more precise, we will perturb the electrode configuration of CEM by $F \in \mathcal{G}^1(\Omega)$ and study the corresponding forward solutions parametrized by $h = F - \mathrm{id}$ as h tends to zero in the topology of $C_0^1(\mathbb{R}^n, \mathbb{R}^n)$. We will start by introducing the perturbed setting and considering related variational problems. Subsequently, we will present a *formal* Fréchet derivative of the forward solution with respect to h. Finally, different ways of approximating such a formal derivative will be considered.

5.1. Perturbation by a general diffeomorphism. Let $F \in \mathcal{G}^1(\Omega)$ be arbitrary and denote $h = F - \mathrm{id}$. The forward problem in the corresponding perturbed measurement setting (cf. (2.2)) is to find $(u[h], U[h]) \in \mathcal{H}^1$ that satisfies weakly

$$\begin{aligned}
&\nabla \cdot \sigma \nabla u[h] = 0 && \text{in } \Omega,\\
&\nu \cdot \sigma \nabla u[h] = 0 && \text{on } \partial\Omega \setminus F(\overline{E}),\\
&u[h] + z_m \nu \cdot \sigma \nabla u[h] = U_m[h] && \text{on } F(E_m), \quad m = 1, \dots, M,\\
&\int_{F(E_m)} \nu \cdot \sigma \nabla u[h]\, dS = I_m, && m = 1, \dots, M,
\end{aligned} \tag{5.3}$$

where $I \in \mathbb{C}^M_\diamond$ is a given electrode net current pattern. In particular, it is assumed that the conductivity, the contact impedances and the net currents through the electrodes remain constant under the perturbation F; in effect, F is just regarded as a tool for moving and deforming the electrodes.

Remark 2. *Notice that in this section the pair $(u[h], U[h])$ denotes the solution to the CEM forward problem when the base electrodes $\{E_m\}_{m=1}^M$ are replaced by $\{F(E_m)\}_{m=1}^M$, where $F = \mathrm{id} + h \in \mathcal{G}^1(\Omega)$, while a similar notation, namely $(u[a], U[a])$, was used in Section 4 for the solution of the CEM forward problem with the perturbed electrodes defined by $a \in \mathcal{B}_d \subset C^1(\partial E, \mathbb{R}^n)$ in the sense of Proposition 3.1. In consequence, the functional dependence of $(u[\,\cdot\,], U[\,\cdot\,])$ on the variable in the brackets may vary from one occasion to the next. Be that as it may, the correct interpretation should be obvious given the context, especially because a always denotes an element of $C^1(\partial E, \mathbb{R}^n)$ and h an element of $\mathcal{G}^1(\Omega) - \mathrm{id}$.*

Let $F^* \colon H^1(\Omega) \to H^1(\Omega)$ be the pullback operator defined by $F^* v = v \circ F|_\Omega$; it is easy to see that F^* is a linear isomorphism. Considering the weak formulation of (5.3), cf. (2.3), the chain rule and the substitution of variables induced by F lead easily to the variational equation

$$B^*[h]\big\{(F^* u[h], U[h]), (v, V)\big\} = \sum_{m=1}^M I_m \overline{V}_m \qquad \text{for all } (v, V) \in \mathcal{H}^1, \tag{5.4}$$

where $B^*[h] : \mathcal{H}^1 \times \mathcal{H}^1 \to \mathbb{C}$ is defined via (cf., e.g., [20])

$$B^*[h]\big\{(w,W),(v,V)\big\} = \int_\Omega J_F^{-1}(F^*\sigma)(J_F^{-1})^{\mathrm{T}}\nabla w \cdot \nabla \overline{v}\, |J_F|\, dx + \sum_{m=1}^{M} \frac{1}{z_m}\int_{E_m} \big(W_m - w\big)\big(\overline{V}_m - \overline{v}\big)\, |\mathrm{Jac}\, F|\, dS.$$

Here, J_F is the Jacobian matrix of F, $|J_F|$ is the absolute value of its determinant, and $|\mathrm{Jac}\, F|$ is the surface Jacobian determinant of the restriction $F|_{\partial\Omega} : \partial\Omega \to \partial\Omega$. It follows, e.g., from the unique solvability of (5.3) that $(F^*u[h], U[h]) \in \mathcal{H}^1$ is the unique solution of (5.4).

5.2. Formal derivative of $(F^*u[h], U[h])$. Let us next consider how the modified perturbed solution $(F^*u[h], U[h]) \in \mathcal{H}^1$ approaches $(u,U) \in \mathcal{H}^1$ as $h \in \mathcal{G}^1(\Omega) - \mathrm{id} \subset C_0^1(\mathbb{R}^n,\mathbb{R}^n)$ tends to zero. As a consequence of (2.3) and (5.4), the difference $(F^*u[h], U[h]) - (u,U) \in \mathcal{H}^1$ satisfies the relation

$$\begin{aligned} B\big\{(F^*u[h]-u,\, U[h]-U),(v,V)\big\} &= \int_\Omega \big(\sigma - |J_F|\, J_F^{-1}(F^*\sigma)(J_F^{-1})^{\mathrm{T}}\big)\nabla(F^*u[h])\cdot\nabla\overline{v}\, dx \\ &\quad + \sum_{m=1}^{M}\frac{1}{z_m}\int_{E_m}(U_m[h] - F^*u[h])(\overline{V}_m - \overline{v})\,(1-|\mathrm{Jac}\, F|)\, dS \end{aligned} \tag{5.5}$$

for all $(v,V) \in \mathcal{H}^1$. Our aim is to study the asymptotic behavior of the terms on the right-hand side of (5.5) as $\|h\|_{C^1}$ tends to zero. In what follows, $h_\nu = (h|_{\partial\Omega}\cdot\nu)\nu$ and $h_\tau = h|_{\partial\Omega} - h_\nu$ are the normal and tangential components of $h|_{\partial\Omega}$, respectively; this same notation is also used for other vector fields living on $\partial\Omega$.

LEMMA 5.2. *Let $F = \mathrm{id} + h \in \mathcal{G}^1(\Omega)$. Then, the equalities*

$$J_F^{-1} = \mathbb{I} - J_h, \quad |J_F| = 1 + \nabla\cdot h, \quad |\mathrm{Jac}\, F| = 1 + \mathrm{Div}\, h_\tau, \quad (F^*\sigma)_{ij} = \sigma_{ij} + h\cdot\nabla\sigma_{ij}$$

hold modulo $O(\|h\|_{C^1}^2)$ as h goes to zero in the topology of $C_0^1(\mathbb{R}^n,\mathbb{R}^n)$. Here, $\mathbb{I} \in \mathbb{R}^{n\times n}$ is the identity matrix and Div *is the surface divergence operator (cf., e.g., [6, 9]).*

Proof. The assertion follows from the material in [25, 13, 14], after noting that the normal component h_ν is of the order $O(\|h\|_{C^1}^2)$ because $h|_{\partial\Omega}$ is the difference between two diffeomorphisms on $\partial\Omega$ (cf. [26]). ∎

With (5.5) in mind, we obtain due to Lemma 5.2 that

$$\sigma - |J_F|\, J_F^{-1}(F^*\sigma)(J_F^{-1})^{\mathrm{T}} = \sigma J_h^{\mathrm{T}} + J_h\sigma - (h\cdot\nabla + \nabla\cdot h)\,\sigma + O\left(\|h\|_{C^1}^2\right), \tag{5.6}$$

$$1 - |\mathrm{Jac}\, F| = -\mathrm{Div}\, h_\tau + O\left(\|h\|_{C^1}^2\right), \tag{5.7}$$

where $h\cdot\nabla\sigma$ is defined as the matrix $(h\cdot\nabla\sigma_{ij})_{i,j=1}^n$. Following the line of reasoning in, e.g., [18, Proof of Lemma 3.8], the combination of (5.5) and Proposition 2.1 thus provides us with a preliminary convergence result.

COROLLARY 5.3. *Let $(u,U) \in \mathcal{H}^1$ be the background solution and $(F^*u[h], U[h]) \in \mathcal{H}^1$ the unique solution of* (5.4)*. Then,*

$$\|(F^*u[h], U[h]) - (u,U)\|_{\mathcal{H}^1} \leq C|I|\|h\|_{C^1(\mathbb{R}^n,\mathbb{R}^n)} \tag{5.8}$$

for some $C > 0$ that can be chosen independently of $I \in \mathbb{C}_\diamond^M$ and $h \in \mathcal{G}^1(\Omega) - \mathrm{id}$.

Motivated by (5.5), (5.6) and (5.7), we next consider the functional

$$\Lambda[h](v,V) = \int_\Omega \left(\sigma J_h^{\mathrm{T}} + J_h\sigma - (h\cdot\nabla + \nabla\cdot h)\,\sigma\right)\nabla u\cdot\nabla\overline{v}\,dx \\ - \sum_{m=1}^{M}\frac{1}{z_m}\int_{E_m}\left(U_m - u\right)\left(\overline{V}_m - \overline{v}\right)\,\mathrm{Div}\,h_\tau\,dS, \tag{5.9}$$

which depends linearly on $h \in C_0^1(\mathbb{R}^n,\mathbb{R}^n)$. By using similar techniques as in [17, Lemma 2.5], it is easy to see that

$$|\Lambda[h](v,V)| \le C(\Omega,\sigma,z)|I|\|h\|_{C^1(\mathbb{R}^n,\mathbb{R}^n)}\|(v,V)\|_{\mathcal{H}^1}, \tag{5.10}$$

which, in particular, means that $\Lambda[h]$ is a continuous antilinear functional with respect to $(v,V)\in\mathcal{H}^1$. Hence, by virtue of the Lax–Milgram lemma, there exists a unique $(w[h],W[h])\in\mathcal{H}^1$ such that

$$B\big\{(w[h],W[h]),(v,V)\big\} = \Lambda[h](v,V) \tag{5.11}$$

for all $(v,V)\in\mathcal{H}^1$. The following proposition states, in essence, that this solution is a first order approximation of the difference $(F^*u[h],U[h])-(u,U)\in\mathcal{H}^1$ with respect to $h = F - \mathrm{id}$ for $F\in\mathcal{G}^1(\Omega)$.

Proposition 5.4. *Let $(u,U)\in\mathcal{H}^1$ be the background solution, and $(F^*u[h],U[h])\in\mathcal{H}^1$ and $(w[h],W[h])\in\mathcal{H}^1$ the unique solutions of* (5.4) *and* (5.11)*, respectively. Then, the estimate*

$$\|(F^*u[h]-u,U[h]-U)-(w[h],W[h])\|_{\mathcal{H}^1}\le C|I|\|h\|^2_{C^1(\mathbb{R}^n,\mathbb{R}^n)}$$

holds with $C>0$ that can be chosen independently of $I\in\mathbb{C}^M_\diamond$ and $h\in\mathcal{G}^1(\Omega)-\mathrm{id}$.

Proof. By subtracting (5.5) and (5.11) and making a few estimates based on the Schwarz inequality, (5.6) and (5.7), cf., e.g., [17, Lemma 2.5], one sees that

$$\begin{aligned}\big|B\big\{(F^*u[h]-u-w[h],U[h]-U-W[h]),(v,V)\big\}\big| \\ &\le C\|h\|_{C^1}\|(F^*u[h]-u,U[h]-U)\|_{\mathcal{H}^1}\|(v,V)\|_{\mathcal{H}^1} \\ &\quad + C\|h\|^2_{C^1}\|(F^*u[h],U[h])\|_{\mathcal{H}^1}\|(v,V)\|_{\mathcal{H}^1} \\ &\le C|I|\|h\|^2_{C^1}\|(v,V)\|_{\mathcal{H}^1},\end{aligned} \tag{5.12}$$

where the second step is due to Corollary 5.3 and (2.6). The claim now follows from the coercivity of B via the choice $(v,V)=(F^*u[h]-u-w[h],U[h]-U-W[h])\in\mathcal{H}^1$. ∎

5.3. A 'tangential approximation' of the formal derivative $(w[h],W[h])$. At first glance it may seem as if Proposition 5.4 shows that the mapping $\mathcal{G}^1(\Omega)-\mathrm{id}\ni h\mapsto(F^*u[h],U[h])\in\mathcal{H}^1$ is Fréchet differentiable at the origin with the corresponding derivative being defined by the formally linear mapping $h\mapsto(w[h],W[h])$. Unfortunately, this is not the case because $\mathcal{G}^1(\Omega)-\mathrm{id}$ is not itself a linear space. Our first step toward getting rid of this nuisance is to show that $(w[h],W[h])$ does not change significantly if $h\in\mathcal{G}^1(\Omega)-\mathrm{id}$ is replaced by a suitable vector field that is tangential on $\partial\Omega$. (If you take a linear combination of two tangential fields on $\partial\Omega$ the result is still a tangential vector field, but a linear combination of boundary restrictions of two

elements of $\mathcal{G}^1(\Omega) - \mathrm{id}$ is not in general related to any perturbation in $\mathcal{G}^1(\Omega) - \mathrm{id}$.) We start with a simple lemma.

LEMMA 5.5. *For any $h = F - \mathrm{id}$ with $F \in \mathcal{G}^1(\Omega)$, there exists a vector field $b = b[h] \in C_0^1(\mathbb{R}^n, \mathbb{R}^n)$ such that*

$$b|_{\partial\Omega} = h_\tau \qquad \text{and} \qquad \|h - b\|_{C^1(\mathbb{R}^n,\mathbb{R}^n)} \leq C\|h\|^2_{C^1(\mathbb{R}^n,\mathbb{R}^n)},$$

for some $C > 0$ that can be chosen independently of h.

Proof. To begin with, we note that a straightforward but tedious calculation in local coordinates shows that $h_\nu = h|_{\partial\Omega} - h_\tau \in C^1(\partial\Omega, \mathbb{R}^n)$ satisfies (cf., e.g., [26])

$$\|h_\nu\|_{C^1(\partial\Omega,\mathbb{R}^n)} \leq C\|h\|^2_{C^1(\partial\Omega,\mathbb{R}^n)}, \tag{5.13}$$

where the constant $C > 0$ is independent of $h \in \mathcal{G}^1(\Omega) - \mathrm{id}$. We extend h_ν as a $C_0^1(\mathbb{R}^n, \mathbb{R}^n)$ vector field to the whole of $\mathbb{R}^n$ in such a way that the extension (still) satisfies (5.13) with the norm of $C^1(\partial\Omega, \mathbb{R}^n)$ on the left-hand side replaced by that of $C_0^1(\mathbb{R}^n, \mathbb{R}^n)$ (cf., e.g., [9, Chapter 7, Section 3.1]). Finally, we set $b[h] = h - h_\nu$, which obviously fulfills the requirements of the lemma. ∎

Let $(w[b], W[b]) \in \mathcal{H}^1$ be the unique solution of the variational problem

$$B\big\{(w[b], W[b]), (v, V)\big\} = \Lambda[b](v, V) \qquad \text{for all } (v, V) \in \mathcal{H}^1, \tag{5.14}$$

where $\Lambda[b]$ is defined in the natural way, i.e., by (5.9) after replacing h with $b = b[h]$ of Lemma 5.5. The unique solvability of (5.14) follows from exactly the same line of reasoning as that of (5.11). The following lemma shows, in essence, that the statement of Proposition 5.4 remains valid if $(w[h], W[h])$ is replaced by $(w[b], W[b])$.

LEMMA 5.6. *Let $(w[h], W[h]), (w[b], W[b]) \in \mathcal{H}^1$ be the unique solutions of* (5.11) *and* (5.14)*, respectively. Then, it holds that*

$$\|(w[h], W[h]) - (w[b], W[b])\|_{\mathcal{H}^1} \leq C|I|\|h\|^2_{C^1(\mathbb{R}^n,\mathbb{R}^n)},$$

where the constant $C > 0$ can be chosen independently of $I \in \mathbb{C}^M_\diamond$ and $h \in \mathcal{G}^1(\Omega) - \mathrm{id}$.

Proof. Because of the coercivity of B, we have

$$\begin{aligned}
&\|(w[h], W[h]) - (w[b], W[b])\|^2_{\mathcal{H}^1} \\
&\quad \leq C|B\{(w[h], W[h]) - (w[b], W[b]), (w[h] - w[b], W[h] - W[b])\}| \\
&\quad = C\,|\Lambda[h](w[h] - w[b], W[h] - W[b]) - \Lambda[b](w[h] - w[b], W[h] - W[b])| \\
&\quad \leq C\,|I|\,\|h - b\|_{C^1}\|(w[h], W[h]) - (w[b], W[b])\|_{\mathcal{H}^1} \\
&\quad \leq C\,|I|\,\|h\|^2_{C^1}\|(w[h], W[h]) - (w[b], W[b])\|_{\mathcal{H}^1},
\end{aligned}$$

where the second to last inequality follows from the linearity of $\Lambda[\,\cdot\,]$ and the same estimates that led to (5.10), and the last step is a consequence of Lemma 5.5. ∎

5.4. Smooth approximations of $(w[b], W[b])$. In Section 6, we will show that after replacing the general diffeomorphism $F \in \mathcal{G}^1(\Omega)$ in the above analysis by the one introduced in Proposition 3.1 and Theorem 5.1, i.e., by $F = F[a] = \mathrm{id} + h[a]$, the unique solution $(u'[a], U'[a]) \in \mathcal{H}^{1-\varepsilon}$ of the derivative problem (4.1) can be obtained by modifying the first component of $(w[b], W[b])$, where $b = b[h[a]]$, in a suitable way. This process involves including a directional derivative of the interior potential

component of the background solution $(u, U) = (u[0], U[0]) \in \mathcal{H}^1$ as an argument of the sesquilinear form $B : \mathcal{H}^1 \times \mathcal{H}^1 \to \mathbb{C}$. Unfortunately, according to Remark 1, the derivatives of u are merely in $H^{1-\epsilon}(\Omega)$, and thus such analysis cannot be carried out without suitable modifications. For this reason, we introduce a sequence of smooth approximations for $u \in H^{2-\epsilon}(\Omega)/\mathbb{C}$, and subsequently also for $(w[b], W[b]) \in \mathcal{H}^1$.

Since $C^\infty(\partial\Omega)$ is dense in $H^s(\partial\Omega)$ for arbitrary $s \in \mathbb{R}$ (see, e.g., [29]), one may pick a sequence of smooth and mean-free current patterns $\{f^{(j)}\}_{j=1}^\infty \subset C^\infty(\partial\Omega)$ that converge to $\nu\cdot\sigma\nabla u|_{\partial\Omega}$ in $H^{1/2-\epsilon}(\partial\Omega)$, $\epsilon > 0$, as $j \in \mathbb{N}$ tends to infinity (see Remark 1); observe that $\nu\cdot\sigma\nabla u|_{\partial\Omega}$ also has vanishing mean due to the Gauss divergence theorem. Let us denote by $u^{(j)} \in C^\infty(\overline{\Omega})/\mathbb{C}$ the solution of

$$\nabla\cdot\sigma\nabla u^{(j)} = 0 \quad \text{in } \Omega, \qquad \nu\cdot\sigma\nabla u^{(j)} = f^{(j)} \quad \text{on } \partial\Omega. \tag{5.15}$$

It follows from the well posedness of the Neumann problem (5.15), cf. [29, Chapter 2, Remark 7.2], that

$$\lim_{j\to\infty} u^{(j)} = u \qquad \text{in } H^{2-\epsilon}(\Omega)/\mathbb{C}. \tag{5.16}$$

We denote by $(w^{(j)}[b], W^{(j)}[b]) \in \mathcal{H}^1$ the solution of the variational equation

$$B\big\{(w^{(j)}[b], W^{(j)}[b]), (v, V)\big\} = \Lambda_j[b](v, V) \qquad \text{for all } (v, V) \in \mathcal{H}^1. \tag{5.17}$$

Here, the antilinear functional $\Lambda_j[b] : \mathcal{H}^1 \to \mathbb{C}$ is defined via replacing $(u, U) \in \mathcal{H}^1$ by $(u^{(j)}, U^{(j)}) \in \mathcal{H}^1$ in the expression defining $\Lambda[b]$, with $U^{(j)} \in \mathbb{C}^M/\mathbb{C}$ defined component-wise as

$$U_m^{(j)} = \frac{1}{|E_m|}\Big(z_m \int_{E_m} f^{(j)}\, dS + \int_{E_m} u^{(j)}\, dS\Big), \qquad m = 1, \dots, M. \tag{5.18}$$

According to the following lemma, as j goes to infinity $(w^{(j)}[b], W^{(j)}[b])$ tends to $(w[b], W[b])$.

LEMMA 5.7. *The variational problem* (5.17) *is uniquely solvable in* $\mathcal{H}^1$. *The corresponding solution* $(w^{(j)}[b], W^{(j)}[b]) \in \mathcal{H}^1$ *converges to* $(w[b], W[b])$ *in* $\mathcal{H}^1$ *as* $j \in \mathbb{N}$ *tends to infinity.*

Proof. To begin with, let us consider the connection between $U^{(j)}$ and U. Integrating the third equation of (2.2) over E_m results in

$$U_m = \frac{1}{|E_m|}\Big(z_m \int_{E_m} \nu\cdot\sigma\nabla u\, dS + \int_{E_m} u\, dS\Big), \qquad m = 1, \dots, M.$$

Thus, it can easily be concluded from (5.18), (5.16) and the trace theorem that $(u^{(j)}, U^{(j)})$ converges to (u, U) in $\mathcal{H}^1$. On the other hand, the estimate

$$|\Lambda[b](v, V) - \Lambda_j[b](v, V)| \le C\|(u, U) - (u^{(j)}, U^{(j)})\|_{\mathcal{H}^1}\|b\|_{C^1(\mathbb{R}^n, \mathbb{R}^n)}\|(v, V)\|_{\mathcal{H}^1} \tag{5.19}$$

follows in exactly the same way as (5.10). Note that (5.19) and the triangle inequality also show the (uniform) boundedness of the antilinear functional $\Lambda_j[b] : \mathcal{H}^1 \to \mathbb{C}$, as the boundedness of $\Lambda[b] : \mathcal{H}^1 \to \mathbb{C}$ was, in essence, established already by (5.10).

Now, the unique solvability of (5.17) follows from the Lax–Milgram lemma. Moreover, by definition

$$B\big\{\big((w[b], W[b]) - (w^{(j)}[b], W^{(j)}[b])\big), (v, V)\big\} = \Lambda[b](v, V) - \Lambda_j[b](v, V),$$

and so the convergence of $(w^{(j)}[b], W^{(j)}[b])$ towards $(w[b], W[b])$ in $\mathcal{H}^1$ follows from (5.19) and the coercivity of B via the choice $(v, V) = (w[b] - w^{(j)}[b], W[b] - W^{(j)}[b]) \in \mathcal{H}^1$. ∎

6. Proof of the main results. Let $a \in \mathcal{B}_d \subset C^1(\partial E, \mathbb{R}^n)$, with $d > 0$ as in Theorem 5.1, be a vector field defining the perturbation of the electrode boundaries in the sense of Section 3, and $F[a] \in \mathcal{G}^1(\Omega)$ the corresponding diffeomorphism guaranteed by Theorem 5.1. We denote $h = h[a] = F[a] - \mathrm{Id} \in C_0^1(\mathbb{R}^n, \mathbb{R}^n)$, and let $b = b[h[a]] \in C_0^1(\mathbb{R}^n, \mathbb{R}^n)$ be the vector field of Lemma 5.5 corresponding to $h[a]$. In particular, on $\partial\Omega$ we have $b = h_\tau$, and on ∂E it also holds that $b = a_\tau$; see the proof of Proposition 3.1.

With the help of $(w[b], W[b]) \in \mathcal{H}^1$ and $(w^{(j)}[b], W^{(j)}[b]) \in \mathcal{H}^1$, as defined in Sections 5.3 and 5.4, respectively, and corresponding to $b = b[h[a]]$, we define the potentials

$$\tilde{w}[b] = w[b] - b \cdot \nabla u, \qquad \tilde{w}^{(j)}[b] = w^{(j)}[b] - b \cdot \nabla u^{(j)}, \quad j = 1, 2, \ldots, \tag{6.1}$$

where $u^{(j)} \in C^\infty(\overline{\Omega})/\mathbb{C}$ is as in Section 5.4. By (5.16) and Lemma 5.7, we observe that

$$\lim_{j\to\infty} (\tilde{w}^{(j)}[b], W^{(j)}[b]) = (\tilde{w}[b], W[b]) \tag{6.2}$$

in $\mathcal{H}^{1-\varepsilon}$ for any $\epsilon > 0$ (cf. [29, Chapter 1, Proposition 12.1]). In what follows, we will show that $(\tilde{w}[b], W[b]) \in \mathcal{H}^{1-\varepsilon}$ is the unique solution of (4.1) for $a \in \mathcal{B}_d$. In particular, the pair $(\tilde{w}[b], W[b])$ turns out to depend only on $a \in \mathcal{B}_d$, not on its 'extensions' $h = h[a] \in \mathcal{G}^1(\Omega) - \mathrm{id}$ and $b = b[h[a]] \in C_0^1(\mathbb{R}^n, \mathbb{R}^n)$.

THEOREM 6.1. *For any $a \in C^1(\partial E, \mathbb{R}^n)$ the boundary value problem (4.1) has a unique solution $(u'[a], U'[a]) \in \mathcal{H}^{1-\varepsilon}$, $\epsilon > 0$. Moreover, if $a \in \mathcal{B}_d$, then this solution can be given as $(u'[a], U'[a]) = (\tilde{w}[b], W[b])$.*

Proof. (1) Let us tackle the uniqueness first. Take two solutions of (4.1) and abbreviate their difference simply by $(v, V) \in \mathcal{H}^{1-\varepsilon}$. Due to the linearity of (4.1), we have

$$\begin{aligned} &\nabla \cdot \sigma \nabla v = 0 && \text{in } \Omega, \\ &\nu \cdot \sigma \nabla v - \sum_{m=1}^{M} \frac{\chi_m}{z_m}(V_m - v) = 0 && \text{on } \partial\Omega, \\ &\int_{E_m} (V_m - v)\, dS = 0, && m = 1, \ldots, M. \end{aligned} \tag{6.3}$$

Since $v|_{\partial\Omega} \in H^{1/2-\epsilon}(\partial\Omega)/\mathbb{C}$ by the trace theorem, the second and third equalities of (6.3) imply that $\nu \cdot \sigma \nabla v|_{\partial\Omega}$ belongs to $L^2(\partial\Omega)$ and has zero mean. In consequence, it follows from [29, Chapter 2, Remark 7.2] that $v \in H^{3/2}(\Omega)/\mathbb{C}$, which means, in particular, that $(v, V) \in \mathcal{H}^1$. By solving the second equation of (6.3) for $V_m - v|_{E_m}$ and substituting into the third equation, we see that (v, V) is the solution of the background problem (2.2) with $I = 0$. Hence, the unique solvability of (2.2) tells us that (v, V) is the zero element of $\mathcal{H}^1$, and thus also that of $\mathcal{H}^{1-\varepsilon}$.

(2) Before proving the existence, we consider what kinds of variational equations $(\tilde{w}^{(j)}[b], W^{(j)}[b]) \in \mathcal{H}^1$ satisfies. To this end, let $\varphi \in C^\infty(\overline{\Omega})$ and $V \in \mathbb{C}^M$ be arbitrary.

By (6.1) and the definition of $(w^{(j)}[b], W^{(j)}[b]) \in \mathcal{H}^1$, we have

$$\begin{aligned} B\big\{(\tilde{w}^{(j)}[b], W^{(j)}[b]), (\varphi, V)\big\} = &\int_\Omega \big(\sigma J_b^{\mathrm{T}} + J_b \sigma - (b\cdot\nabla + \nabla\cdot b)\,\sigma\big)\,\nabla u^{(j)}\cdot\nabla\overline{\varphi}\,dx \\ &- \int_\Omega \sigma\nabla(b\cdot\nabla u^{(j)})\cdot\nabla\overline{\varphi}\,dx \\ &- \sum_{m=1}^M \frac{1}{z_m}\int_{E_m} \big(U_m^{(j)} - u^{(j)}\big)\,\big(\overline{V}_m - \overline{\varphi}\big)\,\mathrm{Div}\,b\,dS \\ &+ \sum_{m=1}^M \frac{1}{z_m}\int_{E_m} \big(b\cdot\nabla u^{(j)}\big)\,\big(\overline{V}_m - \overline{\varphi}\big)\,dS. \end{aligned}$$

Standard vector calculus, the divergence theorem and the fact that b is tangential on $\partial\Omega$ allow us to transform the volume integrals into one boundary integral (cf., e.g., [20]):

$$\begin{aligned} B\big\{(\tilde{w}^{(j)}[b], W^{(j)}[b]), (\varphi, V)\big\} = &\int_{\partial\Omega} \big(\nu\cdot\sigma\nabla u^{(j)}\big)\big(b\cdot\nabla\overline{\varphi}\big)\,dS \\ &- \sum_{m=1}^M \frac{1}{z_m}\int_{E_m} \big(U_m^{(j)} - u^{(j)}\big)\,\big(\overline{V}_m - \overline{\varphi}\big)\,\mathrm{Div}\,b\,dS \\ &+ \sum_{m=1}^M \frac{1}{z_m}\int_{E_m} \big(b\cdot\nabla u^{(j)}\big)\,\big(\overline{V}_m - \overline{\varphi}\big)\,dS. \end{aligned}$$

Furthermore, due to the properties of the surface gradient Grad (cf. [6, 9]), it follows that

$$\begin{aligned} B\big\{(\tilde{w}^{(j)}[b], W^{(j)}[b]), (\varphi, V)\big\} = &\int_{\partial\Omega\setminus\overline{E}} \big(\nu\cdot\sigma\nabla u^{(j)}\big)\big(b\cdot\nabla\overline{\varphi}\big)dS \\ &- \sum_{m=1}^M \int_{E_m} \big(\nu\cdot\sigma\nabla u^{(j)}\big)\big(b\cdot\mathrm{Grad}\,\big(\overline{V}_m - \overline{\varphi}\big)\big)dS \\ &- \sum_{m=1}^M \frac{1}{z_m}\int_{E_m} \big(U_m^{(j)} - u^{(j)}\big)\,\big(\overline{V}_m - \overline{\varphi}\big)\,\mathrm{Div}\,b\,dS \\ &- \sum_{m=1}^M \frac{1}{z_m}\int_{E_m} b\cdot\mathrm{Grad}\big(U_m^{(j)} - u^{(j)}\big)\,\big(\overline{V}_m - \overline{\varphi}\big)\,dS. \end{aligned} \tag{6.4}$$

Now, the limit (5.16), the trace theorem, the boundedness of the surface gradient, say, from $H^{3/2-\epsilon}(\partial\Omega)$ to $[H^{1/2-\epsilon}(\partial\Omega)]^n$, and the second and third equation of (2.2) straightforwardly yield

$$\begin{aligned} \lim_{j\to\infty} B\big\{(\tilde{w}^{(j)}[b], W^{(j)}[b]), (\varphi, V)\big\} &= -\sum_{m=1}^M \frac{1}{z_m}\int_{E_m} \mathrm{Div}\big(b\,(U_m - u)(\overline{V}_m - \overline{\varphi})\big)dS \\ &= -\sum_{m=1}^M \frac{1}{z_m}\int_{\partial E_m} (a_\tau\cdot\nu_{\partial E})\big(U_m - u\big)\big(\overline{V}_m - \overline{\varphi}\big)ds, \end{aligned} \tag{6.5}$$

where the second step follows from the divergence theorem for surfaces and the fact that $b[a] = (h[a])_\tau = a_\tau$ on ∂E by the construction.

(3) Let us then prove that $(\tilde{w}[b], W[b]) \in \mathcal{H}^{1-\varepsilon}$ is a solution of (4.1) if $a \in \mathcal{B}_d$, i.e., when $h[a] = F[a] - \mathrm{id}$ and the corresponding $b[h[a]]$ of Lemma 5.5 are well defined. Take note that this is, in fact, enough for proving the existence of a solution to (4.1) for a general $a \in C^1(\partial E, \mathbb{R}^n)$ since the 'right-hand side' of (4.1) depends linearly on a.

To tackle the first equality of (4.1), let $V = 0$ and $\varphi \in C_0^\infty(\Omega)$ be arbitrary. According to the definition of the sesquilinear form B, the identity (6.4) and the definition of distributional differentiation (cf., e.g., [7]), it holds that

$$\langle \nabla \cdot \sigma \nabla \tilde{w}^{(j)}[b], \overline{\varphi} \rangle_\Omega = 0. \tag{6.6}$$

As the elliptic differential operator $\nabla \cdot \sigma \nabla \colon H^{1-\epsilon}(\Omega)/\mathbb{C} \to H^{-1-\epsilon}(\Omega)$ is continuous for any ϵ that is not a half integer [29, Chapter 1, Proposition 12.1], we may pass the limit (6.2) inside the brackets of (6.6). Consequently, $\nabla \cdot \sigma \nabla \tilde{w}[b] = 0$ is satisfied in the sense of distributions in Ω.

Assume still that $V = 0$, but this time let $\varphi \in C^\infty(\overline{\Omega})$. The (generalized) Green's formula (cf., e.g., [7, p. 382, Corollary 1]) and (6.6) indicate that

$$B\big\{(\tilde{w}^{(j)}[b], W^{(j)}[b]), (\varphi, 0)\big\} = \langle \nu \cdot \sigma \nabla \tilde{w}^{(j)}[b], \overline{\varphi} \rangle_{\partial\Omega} + \sum_{m=1}^{M} \frac{1}{z_m} \int_{E_m} \big(\tilde{w}^{(j)}[b] - W_m^{(j)}[b]\big) \overline{\varphi}\, dS.$$

Furthermore, according to [29, Chapter 2, Theorem 7.3] the Neumann trace map $v \mapsto \nu \cdot \sigma \nabla v|_{\partial\Omega}$ is well-defined and bounded from the closed subspace

$$\{v \in H^{1-\epsilon}(\Omega)/\mathbb{C} \mid \nabla \cdot \sigma \nabla v = 0\} \subset H^{1-\epsilon}(\Omega)/\mathbb{C}$$

to $H^{-1/2-\epsilon}(\partial\Omega)$. Hence, (6.2) and the trace theorem give

$$\lim_{j\to\infty} B\big\{(\tilde{w}^{(j)}[b], W^{(j)}[b]), (\varphi, 0)\big\} = \langle \nu \cdot \sigma \nabla \tilde{w}[b], \overline{\varphi} \rangle_{\partial\Omega} + \sum_{m=1}^{M} \frac{1}{z_m} \int_{E_m} \big(\tilde{w}[b] - W_m[b]\big) \overline{\varphi}\, dS.$$

But then again, by (6.5) it also holds that

$$\lim_{j\to\infty} B\big\{(\tilde{w}^{(j)}[b], W^{(j)}[b]), (\varphi, 0)\big\} = \sum_{m=1}^{M} \frac{1}{z_m} \langle (a_\tau \cdot \nu_{\partial E})(U_m - u)\delta_m, \overline{\varphi} \rangle_{\partial\Omega}\,.$$

As $C^\infty(\overline{\Omega})|_{\partial\Omega}$ is dense in $H^s(\partial\Omega)$ for any $s \in \mathbb{R}$, this proves that $(\tilde{w}[b], W[b])$ satisfies the second equation of (4.1).

Finally, let us take care of the third condition of (4.1). Fix an integer m between 1 and M, define $V \in \mathbb{C}^M$ to be the mth coordinate vector, and choose $\varphi \equiv 0$. Using the definition of B, (6.5) and (6.2), we deduce that

$$\frac{1}{z_m} \int_{E_m} \big(W_m[b] - \tilde{w}[b]\big) dS = -\frac{1}{z_m} \int_{\partial E_m} (a_\tau \cdot \nu_{\partial E})(U_m - u) ds. \tag{6.7}$$

Since m is arbitrary, this shows that $(\tilde{w}[b], W[b]) \in \mathcal{H}^{1-\varepsilon}$ is a solution to (4.1), and the proof is complete. □

Finally, it is the time to provide proofs for Theorem 4.1 and Corollary 4.2.

Proof of Theorem 4.1. To begin with, note that the operator defined by (4.2) is clearly bilinear as the 'right-hand' side of (4.1) depends linearly on both a and (u, U), and the latter also depends linearly on I. Moreover, by Theorem 6.1 for any $I \in \mathbb{C}^M_\diamond$ and $a \in \mathcal{B}_d$ we have

$$\begin{aligned}\|R[a]I - R[0]I - R'(a,I)]\|_{\mathbb{C}^M/\mathbb{C}} &= \|U[a] - U - W[b]\|_{\mathbb{C}^M/\mathbb{C}} \\ &\leq \|U[a] - U - W[h]\|_{\mathbb{C}^M/\mathbb{C}} + \|W[h] - W[b]\|_{\mathbb{C}^M/\mathbb{C}} \\ &\leq C|I|\|a\|^2_{C^1(\partial E,\mathbb{R}^n)},\end{aligned}$$

where $h = h[a] = F[a] - \mathrm{id}$ and $b = b[h[a]]$ are given by Theorem 5.1 and Lemma 5.5, respectively, and the last step follows from the combination of Theorem 5.1, Proposition 5.4 and Lemma 5.6; note that $U[a] = U[h[a]]$ in the sense of Remark 2. Now, the assertion follows from the definition of the norm of $\mathcal{L}(\mathbb{C}^M_\diamond, \mathbb{C}^M/\mathbb{C})$. □

Proof of Corollary 4.2. Let $(\tilde{u}, \tilde{U}) \in \mathcal{H}^1$ and $\tilde{I} \in \mathbb{C}^M_\diamond$ be as in Corollary 4.2 and consider $a \in \mathcal{B}_d$. Due to Theorems 4.1 and 6.1, the limit (6.2) and the variational formulation (2.3) corresponding to the current pattern $\tilde{I}$, it holds that

$$\sum_{m=1}^M \tilde{I}_m (R'(a,I))_m = \lim_{j\to\infty} \sum_{m=1}^M \tilde{I}_m W_m^{(j)}[b] = \lim_{j\to\infty} B\big\{(\tilde{w}^{(j)}[b], W^{(j)}[b]), (\overline{\tilde{u}}, \overline{\tilde{U}})\big\}. \quad (6.8)$$

On the other hand, following the same line of reasoning as in (6.5) — and approximating $\tilde{u}$ by a sequence of smooth functions $\{\varphi_j\}$ —, we obtain that

$$\lim_{j\to\infty} B\big\{(\tilde{w}^{(j)}[b], W_m^{(j)}[b]), (\overline{\tilde{u}}, \overline{\tilde{U}})\big\} = -\sum_{m=1}^M \frac{1}{z_m} \int_{\partial E_m} (a_\tau \cdot \nu_{\partial E})\big(U_m - u\big)\big(\tilde{U}_m - \tilde{u}\big) ds, \quad (6.9)$$

where the right-hand side is well defined since both $u|_{\partial E}$ and $\tilde{u}|_{\partial E}$ belong to $H^{1-\epsilon}(\partial E)/\mathbb{C}$ because of Remark 1 and the trace theorem. As both the left-hand side of (6.8) and the right-hand side of (6.9) depend linearly on a, the assertion holds, in fact, for any $a \in C^1(\partial E, \mathbb{R}^n)$ and the proof is complete. □

7. Application to conductivity reconstruction. Let us numerically demonstrate that the Fréchet derivative of Theorem 4.1 can be utilized in conductivity reconstruction by minimizing the error appearing due to the incorrect modelling of the electrode locations as a part of a reconstruction algorithm. We consider a simple two-dimensional setting where the object of interest Ω is a disk with radius $\rho > 0$. There are M identical electrodes of length $\lambda > 0$ attached to the boundary $\partial\Omega$. Since the electrode length is fixed, the electrodes are fully parametrized by the set of their initial polar angles $\theta \in \mathbb{R}^M$ (in the counterclockwise direction). The needed forward solutions of (2.2) are computed using a finite element method related to a discretization of Ω into triangles; in the reconstruction algorithm, we look for conductivities of the form $\sigma = \sum_k \sigma_k \varphi_k$, where $\{\sigma_k\} \subset (0, \infty)$ and $\{\varphi_k\}$ is a suitable basis corresponding to the elements in question. In all of our computations, the contact impedances $z_m = 1$, $m = 1, \ldots, M$, are assumed to be known, but we note that their estimations could also be included as a part of the algorithm introduced below (cf. [12, 37]).

In what follows, we outline the ideas behind our reconstruction method, but do not discuss all details about, e.g., the form of the smoothness prior for the conductivity; see, e.g., [21, 22] for more information. Our main aim is not so much to compare the

functionality of our method with reconstruction techniques presented elsewhere, but to make an 'internal' comparison between three cases: (i) the precise locations of the electrodes are known; (ii) the locations of the electrodes are known inaccurately and this is not taken into account in the algorithm; (iii) the locations of the electrodes are known inaccurately, but this information is fine-tuned as a part of the algorithm. We will demonstrate that (i) and (iii) give comparable results, while the quality of reconstructions for (ii) is intolerably bad.

7.1. Bayesian inversion. In the Bayesian approach, all quantities are considered as random variables with some known prior distribution. Combining the information in the prior with the measurement data, one gets the updated posterior distribution for the parameters of interest.

Let $\{I^{(j)}\}_{j=1}^{M-1}$ be a basis of $\mathbb{R}^M_\diamond$. The measured voltages are modeled as

$$V^{(j)} = U^{(j)}(\sigma,\theta) + \eta^{(j)} \in \mathbb{R}^M, \qquad j = 1,\ldots,M-1. \tag{7.1}$$

Here, $(u^{(j)}(\sigma,\theta), U^{(j)}(\sigma,\theta)) \in H^1(\Omega)\oplus\mathbb{R}^M_\diamond$ is the solution of (2.2) for the net electrode current pattern $I^{(j)}$, the (real) conductivity σ and with electrodes parametrized by their initial angles $\theta \in \mathbb{R}^M$ (and assumed not to overlap). Notice that we have fixed the ground level of potential by requiring that $U^{(j)}(\sigma,\theta)$ has vanishing mean. The components of the noise vector $\eta^{(j)} \in \mathbb{R}^M$ are assumed to be independent realizations of zero mean Gaussian random variables. To simplify the notation, we pile the electrode currents, voltages and noise vector into arrays of length $M^2 - M$, i.e., employ the shorthand notations

$$\begin{aligned}
\mathcal{I} &= [(I^{(1)})^{\mathrm{T}},\ldots,(I^{(M-1)})^{\mathrm{T}}]^{\mathrm{T}},\\
\mathcal{V} &= [(V^{(1)})^{\mathrm{T}},\ldots,(V^{(M-1)})^{\mathrm{T}}]^{\mathrm{T}},\\
\eta &= [(\eta^{(1)})^{\mathrm{T}},\ldots,(\eta^{(M-1)})^{\mathrm{T}}]^{\mathrm{T}},\\
\mathcal{U}(\sigma,\theta;\mathcal{I}) &= [(U^{(1)}(\sigma,\theta))^{\mathrm{T}},\ldots,(U^{(M-1)}(\sigma,\theta))^{\mathrm{T}}]^{\mathrm{T}}.
\end{aligned} \tag{7.2}$$

This allows us to write the measurement model as $\mathcal{V} = \mathcal{U}(\sigma,\theta;\mathcal{I}) + \eta \in \mathbb{R}^{M^2-M}$.

The discretized conductivity is given a homogeneous Gaussian smoothness prior with an inverse covariance Γ_σ^{-1} and a positive homogeneous mean $\sigma^\star$; for more details about the construction of smoothness priors, see [22]. To include the control of electrode information in the Bayesian framework, the initial angles are given a Gaussian prior density with an equispaced mean (over one rotation) $\theta^\star \in \mathbb{R}^M$ and a diagonal covariance matrix $\Gamma_\theta = \gamma^2\mathbb{I}$, where $\gamma > 0$ is the corresponding standard deviation. As a result, given a measurement $\mathcal{V} \in \mathbb{R}^{M^2-M}$ of the form (7.1), a *maximum a posteriori* estimate is obtained as a minimizer of the Tikhonov-type functional

$$\begin{aligned}
\Phi(\sigma,\theta) :=\ & (\mathcal{U}(\sigma,\theta;\mathcal{I}) - \mathcal{V})^{\mathrm{T}}\Gamma_\eta^{-1}(\mathcal{U}(\sigma,\theta;\mathcal{I}) - \mathcal{V})\\
&+ (\sigma-\sigma^\star)^{\mathrm{T}}\Gamma_\sigma^{-1}(\sigma-\sigma^\star) + \gamma^{-2}|\theta-\theta^\star|^2,
\end{aligned} \tag{7.3}$$

where Γ_η is the diagonal noise covariance matrix; see [22]. In this work, we do not pay any attention to the unique solvability of this problem, but just implement a straightforward Newton-based algorithm for minimizing Φ.

7.2. Minimization scheme. Our initial guess for the electrode polar angles and the conductivity are

$$\theta^{(0)} = \theta^\star, \qquad \sigma^{(0)} = \sigma^\star, \tag{7.4}$$

respectively, i.e., the mean values of the corresponding prior distributions. You may think that $\theta^\star$ determines the locations where we tried to attach the electrodes but failed for some reason, e.g., due to patient movement, and that $\sigma^\star$ corresponds to a known background conductivity level of the imaged object. We perform the minimization of Φ by the Gauss–Newton method combined with the golden section line search; see [10, 33] for details. To this end, both the Jacobian of $\mathcal{U}(\sigma,\theta;\mathcal{I})$ with respect to σ and the one with respect to θ are required. For the computation of the former, we refer to [21]. By the dual formula (4.3), the latter Jacobian can be sampled via trivial linear algebra (a change of basis) after evaluating the expression

$$\big(u^{(j)}(\sigma,\theta) - U_m^{(j)}(\sigma,\theta)\big)\big(u^{(l)}(\sigma,\theta) - U_m^{(l)}(\sigma,\theta)\big)$$

at the end points of the mth electrode for each triplet of indices (j,l,m), $j,l = 1,\ldots,M-1$ and $m = 1,\ldots,M$. (Notice that in our two dimensional setting the integrals on the right-hand side of (4.3) reduce to point evaluations of the respective integrands at the electrode end points.) In order to compute the Jacobian of $\mathcal{U}(\sigma,\theta;\mathcal{I})$ with respect to θ, we need not solve any extra forward problems since at each iteration step all the pairs $(u^{(j)}(\sigma,\theta), U^{(j)}(\sigma,\theta))$, $j = 1,\ldots,M-1$, must be computed already for evaluating the functional Φ of (7.3).

7.3. Numerical results. The target object for the numerical example has radius $\rho = 2$, $M = 16$ nonuniformly located electrodes of length $\lambda = \pi/10$ on its boundary and a smooth internal conductivity distribution of the form

$$\varsigma(x) = 1 + 2e^{-8|x-x_0|^2},$$

where $x_0 = (0.8, 0.8)$; see Figure 7.1(a) for a visualization of the measurement configuration. Denoting the jth Euclidean basis vector of $\mathbb{R}^M$ by e_j, we simulate the exact data $\mathcal{U}(\varsigma,\theta;\mathcal{I})$ using the input current basis $I^{(j)} = \mathrm{e}_1 - \mathrm{e}_j \in \mathbb{R}^m_\diamond$, $j = 1,\ldots,M-1$ (and a considerably different FEM mesh compared to those employed in the reconstruction algorithm in order to avoid an inverse crime). The actual noisy measurement realization $\mathcal{V}$ is then formed via (7.1) by picking a particular noise component $\eta_m^{(j)}$, $m = 1,\ldots,M$, $j = 1,\ldots,M-1$, from a zero mean Gaussian distribution with variance

$$0.01^2|U_m^{(j)}(\varsigma,\theta)|^2 + 0.001^2 \max_{1\le k,l\le M} |U_k^{(j)}(\varsigma,\theta) - U_l^{(j)}(\varsigma,\theta)|^2, \tag{7.5}$$

where the relation between $\mathcal{U}(\varsigma,\theta;\mathcal{I})$ and $U_m^{(j)}(\varsigma,\theta)$ is as in (7.2). The realization of the noise vector $\eta \in \mathbb{R}^{M^2-M}$ is kept fixed during the numerical tests, in order to allow a fair comparison between different test cases. For further justification of the noise model (7.5), see [20], but anyway notice that (7.5) corresponds to more than one percent of relative noise.

We assume (a bit unrealistically) to know the covariance of the measurement noise, i.e., we use the diagonal covariance matrix defined by the noise model (7.5) as Γ_η in (7.3). We do not elaborate on the choice of Γ_σ in (7.3) in further detail: it originates from a smoothness prior built following the material in [22], with the level of 'smoothing' chosen so that the obtained reconstruction for a *known measurement configuration* is reasonably good (cf. Figure 7.1(b)). Since our aim is to (internally) compare the three cases (i), (ii) and (iii) as explained just before Section 7.1, we do not try optimize the choice of the prior for σ, but emphasize that its is the same throughout the numerical studies. The standard deviation of the prior distribution

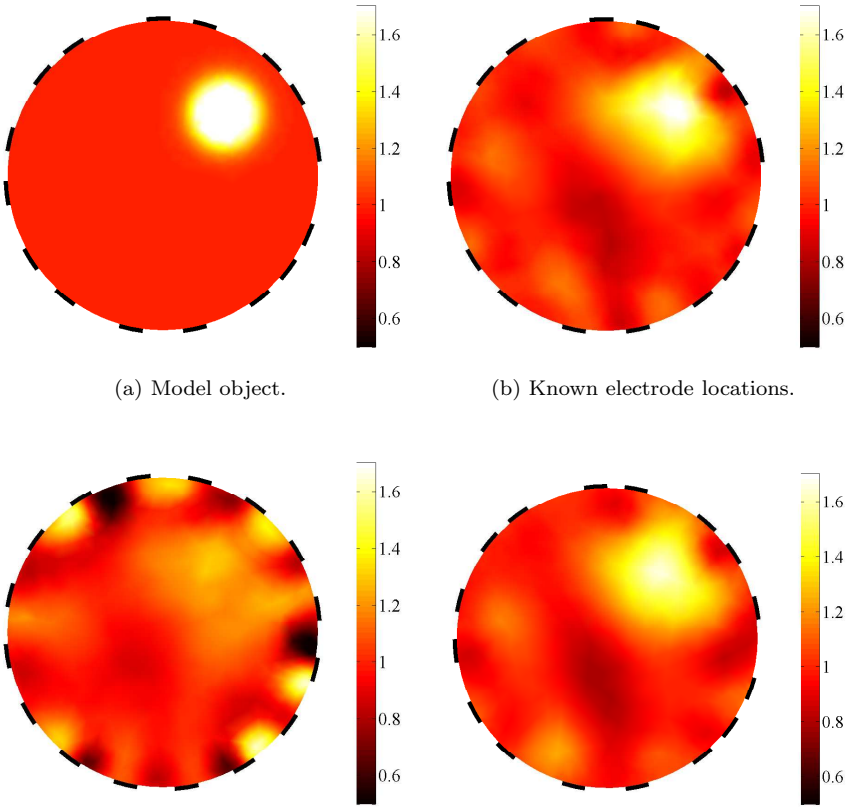

(a) Model object.

(b) Known electrode locations.

(c) Incorrect fixed electrode locations.

(d) Simultaneous retrieval.

Fig. 7.1: Simultaneous reconstruction of the conductivity distribution and the electrode locations compared with results obtained with fixed electrode positions. (See text for further details.)

for the electrode locations was set to $\gamma = \pi/16$, but the algorithm does not seem to be very sensitive with respect to this choice. In particular, we did not experience any overlapping of electrodes due to too low regularization with respect to the electrode locations. All the needed forward solutions of (2.2) were approximated by a finite element method using piecewise quadratic basis functions.

Figure 7.1 illustrates the results provided by our algorithm. The target configuration used in the data simulation is shown in Figure 7.1(a). The reconstruction corresponding to exact knowledge of the electrode locations is depicted in Figure 7.1(b); it was obtained by finding a (local) minimizer for Φ of (7.3) with respect to σ in the case that the last term of Φ is deleted and θ is chosen to be the (fixed) value corresponding to the correct electrode locations shown in Figure 7.1(a). The reconstruction in Figure 7.1(c) was obtained in the same manner, but with the essential difference of assuming the incorrect equispaced locations $\theta = \theta^\star$ for the electrodes. It is obvious that ignoring the incompleteness of the information on the electrode locations results

in severe artefacts in the conductivity reconstruction close to the object boundary. Figure 7.1(d) visualizes simultaneous retrieval of the conductivity distribution and the electrode locations; this reconstruction corresponds to a (local) minimizer of the whole Tikhonov functional (7.3) with respect to both σ and θ, starting from the initial guesses (7.4). Comparing Figure 7.1(d) with Figure 7.1(b) and Figure 7.1(c), it is apparent that the simultaneous retrieval of both the conductivity distribution and the electrode locations results in a qualitatively similar reconstruction as knowing the exact electrode locations to begin with, and in a far better reconstruction than altogether ignoring the inaccuracies in the electrode information.

All reconstructions of Figure 7.1 were obtained by running the Gauss–Newton based minimization scheme until a (local) minimum was reached. The algorithm was applied to a number of different target electrode configurations and conductivity phantoms (with homogeneous backgrounds), resulting almost always in reconstructions qualitatively similar to those presented in Figure 7.1.

8. Concluding remarks. We have presented the Fréchet derivative of the measurement map of practical EIT with respect to the electrode shapes and locations as a part of the solution to a certain elliptic boundary value problem. Through a two-dimensional numerical study based on simulated data, we have demonstrated that incorporating the Fréchet derivative into a Newton–type output least squares reconstruction algorithm in the framework of the CEM of EIT allows simultaneous reconstruction of the conductivity distribution and the electrode locations.

Acknowledgements. We would like to thank Professor Jari Kaipio's research group at the University of Eastern Finland (Kuopio) for letting us use their FEM solver for the CEM.

REFERENCES

[1] D. Barber and B. Brown, *Errors in reconstruction of resistivity images using a linear reconstruction technique*, Clin. Phys. Physiol. Meas., 9 (1988), pp. 101–104.
[2] L. Borcea, *Electrical impedance tomography*, Inverse Problems, 18 (2002), pp. R99–R136.
[3] W. Breckon and M. Pidcock, *Data errors and reconstruction algorithms in electrical impedance tomography*, Clin. Phys. Physiol. Meas., 9 (1988), pp. 105–109.
[4] M. Cheney, D. Isaacson, and J. C. Newell, *Electrical Impedance tomography*, SIAM Rev., 41 (1999), pp. 85–101.
[5] K.-S. Cheng, D. Isaacson, J. S. Newell, and D. G. Gisser, *Electrode models for electric current computed tomography*, IEEE Trans. Biomed. Eng., 36 (1989), pp. 918–924.
[6] D. Colton and R. Kress, *Inverse Acoustic and Electromagnetic Scattering Theory*, Springer-Verlag, Berlin, 1992.
[7] R. Dautray and J-L. Lions, *Mathematical Analysis and Numerical Methods for Science and Technology*, Vol. 2, Springer-Verlag, Berlin, 1988.
[8] J. Dardé, N. Hyvönen, A. Seppänen, and S. Staboulis, *Simultaneous reconstruction of outer boundary shape and admittance distribution in electrical impedance tomography*, in preparation.
[9] M. C. Delfour and J-P. Zolésio, *Shapes and Geometries; Analysis, Differential Calculus and Optimization*, SIAM, 2001.
[10] R. Griesmaier and N. Hyvönen, *A regularized Newton method for locating thin tubular conductivity inhomogeneities*, Inverse Problems, 27, 115008 (2011).
[11] M. Hanke, B. Harrach, and N. Hyvönen, *Justification of point electrode models in electrical impedance tomography*, Math. Models Methods Appl. Sci., 21, 1395-1413 (2011).
[12] L. M. Heikkinen, T. Vilhunen, R. M. West, and M. Vauhkonen, *Simultaneous reconstruction of electrode contact impedances and internal electrical properties: II. Laboratory experiments*, Meas. Sci. Technol., 13 (2002), pp. 1855–1861.
[13] F. Hettlich, *Fréchet derivatives in inverse obstacle scattering*, Inverse Problems, 11 (1995), pp. 371–382.

[14] F. Hettlich, *Fréchet derivatives in inverse obstacle scattering (erratum)*, Inverse Problems, 14 (1998), pp. 209–210.
[15] F. Hettlich and W. Rundell, *The determination of a discontinuity in a conductivity from a single boundary measurement*, Inverse Problems, 14 (1998), pp. 67–82.
[16] L. Horesh, E. Haber, and L. Tenorio, *Optimal Experimental Design for the Large-Scale Nonlinear Ill-Posed Problem of Impedance Imaging* in Large-scale Inverse Problems and Quantification of Uncertainty, editors L. Biegler, G. Biros, O. Ghattas, M. Heinkenschloss, D. Keyes, B. Mallick, Y. Marzouk, L. Tenorio, B. van Bloemen Waanders and K. Willcox, Wiley, 2010.
[17] N. Hyvönen, *Complete electrode model of electrical impedance tomography: Approximation properties and characterization of inclusions*, SIAM J. Appl. Math., 64 (2004), pp. 902–931.
[18] N. Hyvönen, *Frechet derivative with respect to the shape of a strongly convex nonscattering region in optical tomography*, Inverse Problems, 23 (2007), pp. 2249–2270.
[19] N. Hyvönen, H. Hakula, and S. Pursiainen, *Numerical implementation of the factorization method within the complete electrode model of electrical impedance tomography*, Inverse Probl. Imaging, 1 (2007), pp. 299–317.
[20] N. Hyvönen, K. Karhunen, and A. Seppänen, *Frechet derivative with respect to the shape of an internal electrode in electrical impedance tomography*, SIAM J. Appl. Math., 70 (2010), pp. 1878–1898.
[21] J. P. Kaipio, V. Kolehmainen, E. Somersalo, and M. Vauhkonen, *Statistical inversion and Monte Carlo sampling methods in electrical impedance tomography*, Inverse Problems, 16 (2000), pp. 1487–1522.
[22] J. Kaipio and E. Somersalo, *Statistical and Computational Inverse Problems*, Springer, New York, 2005.
[23] V. Kolehmainen, M. Lassas, and P. Ola, *Inverse conductivity problem with an imperfectly known boundary*, SIAM J. Appl. Math., 21 (2005), pp. 365–383.
[24] V. Kolehmainen, M. Vauhkonen, P. A. Karjalainen, and J. P. Kaipio, *Assessment of errors in static electrical impedance tomography with adjacent and trigonometric current patterns*, Physiol. Meas., 18 (1997), pp. 289–303.
[25] A. Kirsch, *The domain derivative and two applications in inverse scattering theory*, Inverse Problems, 9 (1993), pp. 81–96.
[26] R. Kress and D. Colton, *Integral Equation Methods in Scattering Theory*, Wiley, New York, 1983.
[27] A. Lechleiter and A. Rieder, *Newton regularizations for impedance tomography: A numerical study*, Inverse Problems, 22 (2006), pp. 1967–1987.
[28] A. Lechleiter and A. Rieder, *Newton regularizations for impedance tomography: Convergence by local injectivity*, Inverse Problems, 24 (2008), paper 065009.
[29] J-L. Lions and E. Magenes, *Non-Homogeneous Boundary Value Problems and Applications*, Vol. I, Springer, Berlin, 1972.
[30] A. Nissinen, L. M. Heikkinen , and J. P. Kaipio, *The Bayesian approximation error approach for electrical impedance tomography — experimental results*, Meas. Sci. Technol., 19 (2008), paper 015501.
[31] A. Nissinen, L. M. Heikkinen, V. Kolehmainen, and J. P. Kaipio, *Compensation of errors due to discretization, domain truncation and unknown contact impedances in electrical impedance tomography*, Meas. Sci. Technol., 20 (2009), paper 105504.
[32] A. Nissinen, V. Kolehmainen, and J. P. Kaipio, *Compensation of modelling errors due to unknown domain boundary in electrical impedance tomography*, IEEE Transactions on Medical Imaging, 30 (2011), pp. 231–242.
[33] J. Nocedal and S. J. Wright, *Numerical Optimization*, Springer, New York, 1999.
[34] M. Soleimani, C. Gómez–Laberge, and A. Adler, *Imaging of conductivity changes and electrode movement in EIT*, Physiol. Meas., 27 (2006), pp. S103–S113.
[35] E. Somersalo, M. Cheney, and D. Isaacson, *Existence and uniqueness for electrode models for electric current computed tomography*, SIAM J. Appl. Math., 52 (1992), pp. 1023–1040.
[36] G. Uhlmann, *Electrical impedance tomography and Calderón's problem*, Inverse Problems, 25 (2009), paper 123011.
[37] T. Vilhunen, J. P. Kaipio, P. J. Vauhkonen, T. Savolainen, and M. Vauhkonen, Meas. Sci. Technol., 13 (2002), pp. 1848–1854.